

Pixels or Positions? Benchmarking Modalities in Group Activity Recognition

Drishya Karki¹ Merey Ramazanova¹ Anthony Cioppa² Silvio Giancola¹ Bernard Ghanem¹

¹King Abdullah University of Science and Technology (KAUST), Saudi Arabia

²University of Liège, Belgium

{drishya.karki, merey.ramazanova, silvio.giancola, bernard.ghanem}@kaust.edu.sa
anthony.cioppa@uliege.be

Abstract

Group Activity Recognition (GAR) is well studied on the video modality for surveillance and indoor team sports (e.g., volleyball, basketball). Yet, other modalities such as agent positions and trajectories over time, i.e. tracking, remain comparatively under-explored despite being compact, agent-centric signals that explicitly encode spatial interactions. Understanding whether pixel (video) or position (tracking) modalities leads to better group activity recognition is therefore important to drive further research on the topic. However, no standardized benchmark currently exists that aligns broadcast video and tracking data for the same group activities, leading to a lack of apples-to-apples comparison between these modalities for GAR. In this work, we introduce SoccerNet-GAR, a multimodal dataset built from the 64 matches of the football World Cup 2022. Specifically, the broadcast videos and player tracking modalities for 94,285 group activities are synchronized and annotated with 10 categories. Furthermore, we define a unified evaluation protocol to benchmark two strong unimodal approaches: (i) a competitive video-based classifiers and (ii) a tracking-based classifiers leveraging graph neural networks. In particular, our novel role-aware graph architecture for tracking-based GAR directly encodes tactical structure through positional edges and temporal attention. Our tracking model achieves 67.2% balanced accuracy compared to 58.1% for the best video baseline, while training 4.25 \times faster with 438 \times fewer parameters (197K vs. 86.3M). This study provides new insights into the relative strengths of pixels and positions for group activity recognition. Overall, it highlights the importance of modality choice and role-aware modeling for GAR.

1. Introduction

Group Activity Recognition (GAR) aims to identify collective behaviors that arise from multiple interacting agents

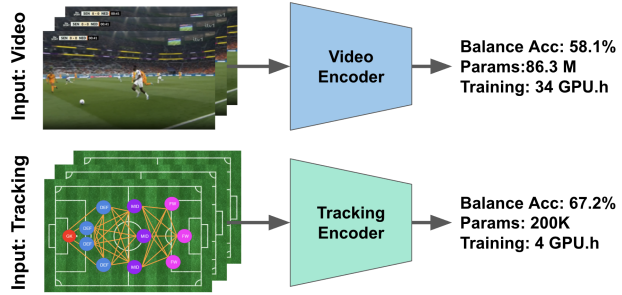


Figure 1. Overview of Our Group Activity Recognition Benchmark. Broadcast video and agent tracking modalities are processed through modality-specific backbones. The resulting representations are evaluated for group activity recognition.

rather than isolated individual actions. This task is central to analytics, automation, and decision support, where understanding both *who* acts as well as *how* agents coordinate over space and time is important. Effective GAR requires modeling individual dynamics together with their spatio-temporal relations at the scene level.

Most contemporary GAR models operate directly on RGB video, which offers appearance, context, and rich semantics. This choice also introduces practical and methodological limitations such as high computational cost, sensitivity to occlusions and editorial cuts, and a tendency to over-rely on appearance cues instead of explicitly modeling interactions. Structured representations based on agent positions and trajectories promise an alternative view that is compact, agent-centric, and efficient to process. Critically, because positions abstract away appearance, they can be *more robust to visual distribution shift* (e.g., cameras, lighting, weather), offering a path toward better generalization across changing conditions. Progress, however, has been hampered by the absence of a standardized benchmark that aligns videos and agent positions per group activity, making apples-to-apples comparisons difficult. Furthermore, principled guidance is lacking for tracking-based GAR on how

to connect agents in a graph and how to aggregate over time.

In this paper, we address these gaps with a unified dataset and evaluation protocol for fair cross-modality evaluation. To do so, we introduce *SoccerNet-GAR*, constructed from the 64 matches of the football World Cup 2022, where broadcast video and agent positions are synchronized at the event level and annotated with 10 group activities. To support this new benchmark, we study two strong *unimodal* approaches: a competitive video-based and a novel role-aware tracking-based classifier leveraging graph neural networks. On the 10-class group activity recognition task, our best tracking model achieves 67.2% balanced accuracy *vs.* 58.1% for the strongest video baseline, while training 4.25 \times faster and using 438 \times fewer parameters.

Contributions. We summarize our contributions as follows: **(i)** We present *SoccerNet-GAR*, a multimodal dataset we curated from 64 football World Cup matches, featuring synchronized broadcast video and tracking data aligned with 94,285 existing event annotations across 10 classes, and split at the match level to enable fair, reproducible evaluation. **(ii)** We propose a *novel role-aware, graph-based classifier* for GAR from tracking data and conduct a comprehensive study of spatial connectivity and temporal aggregation design choices. **(iii)** We establish a *pixels vs. positions* benchmark with identical protocols, report performance and efficiency comparisons, and distill practical design principles for tracking-based GAR. We will release the dataset, evaluation protocol, and method code for transparent comparison and future extensions.

2. Related Work

2.1. Group Activity Recognition

Group Activity Recognition (GAR) studies collective behaviors that arise from coordinated interactions among multiple agents, going beyond single-actor recognition [5]. Early works relied on hand-crafted relational cues and hierarchical temporal models [1, 5, 20]. The field then shifted toward deep learning approaches with graph-based architectures that explicitly encode inter-person dependencies [12, 44, 46], followed by transformer-based methods that model long-range spatial-temporal relationships through self-attention [15, 27]. Popular benchmarks include “Collective Activity” and “Volleyball”, which focus on indoor team sports with controlled camera viewpoints [5, 20].

Contemporary methods predominantly operate on RGB clips using 3D CNNs or vision transformers [33, 34, 37, 38], achieving strong performance but remaining video-centric and compute-intensive. While some works incorporate pose or skeleton cues as auxiliary signals [14, 27], recent studies demonstrate that structured representations alone can achieve competitive results: COMPOSER [47] shows that keypoint-only modality reduces scene biases while main-

taining accuracy, and skeleton-based approaches [28] offer lightweight alternatives that explicitly model spatial relationships. However, these alternative modalities remain comparatively under-explored, and tracking data from sports analytics systems has received limited attention for GAR despite being compact, naturally encoding interactions, and robust to visual distribution shifts. In our work, we address this gap by providing a fair, apples-to-apples evaluation of *unimodal* pixels versus *unimodal* positions under identical protocols with synchronized video and tracking modalities. We propose a study of how positional interactions should be modeled for GAR, demonstrating that tracking-based methods can exceed video-based performance while offering substantial computational advantages.

2.2. Sports Video & Tracking Analytics

Sports video understanding has advanced significantly with broadcast analysis spanning volleyball, basketball, and football. SoccerNet [16] and SoccerNet-v2 [10] established large-scale benchmarks for action spotting, expanding from 3 to 17 action classes with precise temporal annotations. Recent extensions include SoccerNet-v3 [6] with multi-view player localization and tracking annotations, SoccerNet Ball Action Spotting [8] for fine-grained ball interactions, and SoccerNet Game State Reconstruction [36] for end-to-end athlete tracking and identification on minimaps. Action spotting methods have evolved from video-based CNNs to Transformer architectures with self-attention [19, 35, 40, 41], achieving strong temporal localization. However, broadcast video remains sensitive to occlusions, camera edits, zoom variations, and domain shifts across venues and lighting conditions.

Structured tracking signals such as agent centroids, trajectories and skeletons offer a complementary modality with compact representation and improved robustness to visual domain variation. SportsMOT [9] addresses multi-object tracking in dynamic sports scenes, while SportsPose [21] provides large-scale 3D pose annotations. Graph-based methods model agent interactions through node-edge representations, with applications in trajectory prediction [45], pass outcome estimation [13], and event detection [4, 7]. Although both video-based and tracking-based streams have been studied, no prior work provides a direct, fair comparison between broadcast video (pixels) and tracking-derived positions under matched event-level synchronization and match-level splits. In particular, alignment between modalities is often inconsistent, splits are mixed, and graph-based modeling of agent relations from tracking data lacks principled guidance. Our work fills this gap via the introduction of the novel SoccerNet-GAR dataset, in which we provide synchronized broadcast video and tracking data per group activity and establish a unified benchmark comparing pixels and positions with identical evaluation protocols.

2.3. Graph and Relational Modeling

Graph neural networks enable relational reasoning for multi-agent scenes by propagating messages between agents [3, 18, 24, 42]. Spatial-temporal graph models capture inter-person dependencies in human-centric video through sequential message passing [12, 44]. Key design choices concern graph connectivity and temporal aggregation. EdgeConv [39] enables learned, adaptive edges through dynamic neighborhood construction rather than fixed graphs. Training deeper GCNs has been challenging due to oversmoothing, but DeepGCNs [26] demonstrate that residual and dense connections borrowed from CNNs enable 56-layer models with improved performance. Temporal modules range from efficient temporal convolutional networks [25] to recurrent [17] or attention-based aggregators for long-range context [15].

Sports-specific systems show the value of combining detection with relational models. Graph representations naturally capture coordinated play, with recent work applying GNNs to trajectory forecasting [45], action rating [11], and real-time interaction analysis [30]. However, prior studies typically fix parts of the modeling pipeline or evaluate on limited data, making it difficult to extract modality-specific best practices. We complement this literature with a novel role-aware graph classifier for tracking-based GAR and conduct ablations across connectivity schemes (fixed, distance-based, positional edges) and temporal aggregation strategies (pooling, TCN, attention) to identify which design choices yield optimal accuracy-efficiency trade-offs.

3. SoccerNet-GAR Dataset

We present **SoccerNet-GAR**, a new multimodal dataset for Group Activity Recognition constructed from the 64 matches of the football World Cup 2022 tournament. Our dataset was scraped from the PFF FC website [32], which provides comprehensive broadcast videos, player tracking data, and event annotations across all tournament matches. We extend this foundation by creating synchronized temporal windows around each event, enabling direct comparison between video-based and tracking-based approaches for group activity recognition.

3.1. Data Modalities

Our dataset provides two input modalities: broadcast video and player tracking. Both originate from untrimmed full-game broadcast videos of the football World Cup 2022 matches, made publicly available by the PFF FC website.

Video Modality. PFF FC provides the edited broadcast footage at 720p resolution, including multi-view broadcast cameras. Each frame $I_t \in \mathbb{R}^{H \times W \times 3}$ is part of a temporal sequence $\mathbf{X}^V = \{I_t\}_{t=1}^T$ sampled within a temporal window. The video captures appearance cues, scene context,

| Dataset | Year | Domain | Events | Cls. | Mod. |
|----------------------|-------------|-----------------|---------------|-----------|--------------|
| CAD [5] | 2009 | Pedestrian | 2,511 | 5 | V |
| Volleyball [20] | 2016 | Volleyball | 4,830 | 8 | V |
| SoccerNet [16] | 2018 | Football | 6,637 | 3 | V |
| NBA [43] | 2020 | Basketball | 9,172 | 9 | V |
| SoccerNet-v2 [10] | 2021 | Football | 110,458 | 17 | V |
| SoccerNet-BAS [8] | 2024 | Football | 11,041 | 12 | V |
| Café [22] | 2024 | Indoor | 10,297 | 6 | V |
| FIFAWC [31] | 2024 | Football | 5,196 | 12 | V |
| SoccerNet-GAR | 2025 | Football | 94,285 | 10 | V + T |

Table 1. **Comparison of Group Activity Recognition Datasets.** 'V' and 'T' indicate Video and Tracking, respectively. SoccerNet-GAR is the second largest dataset in terms of event and the only one providing synchronized video and tracking modalities.

and visual motion patterns.

Tracking Modality. The tracking data consists of 2D player positions and 3D ball coordinates sampled at 30 fps, automatically extracted from broadcast footage using computer vision tools and manually refined by PFF FC annotators. Player positions span $x \in [-60, 60]\text{m}$, $y \in [-42, 41]\text{m}$; ball positions include height $z \in [-8, 25]\text{m}$. Formally, the tracking input is represented as a temporal sequence of multi-agent states $\mathbf{X}^P = \{\mathcal{S}_t\}_{t=1}^T$, where each state $\mathcal{S}_t = \{s_t^1, \dots, s_t^N\}$ describes N entities (players and ball). Each entity state $s_t^i \in \mathbb{R}^D$ encodes spatial coordinates $(x, y) \in \mathbb{R}^2$ for players and $(x, y, z) \in \mathbb{R}$ for the ball, entity identity, *i.e.* one-hot encoding indicating entity type, and motion dynamics, *i.e.* displacement vectors $(\Delta x, \Delta y)$ capturing movement between consecutive frames.

3.2. Annotation & Modality Alignment

The PFF FC dataset [32] provides event annotations with precise timestamps for each action occurrence. Each event is labeled with one of 10 group activities and temporally marked at the moment of occurrence. Annotations were created by trained annotators and verified through quality control procedures by PFF FC using video and tracking views.

To create our SoccerNet-GAR dataset, we align these event annotations with both input modalities. For each annotated event at timestamp t_e , we extract a temporal window centered at t_e from both the broadcast video and player tracking streams. This alignment process produces synchronized multimodal observations: given an event timestamp, both $\mathbf{X}^V = \{I_t\}_{t=1}^T$ and $\mathbf{X}^P = \{\mathcal{S}_t\}_{t=1}^T$ span the same temporal window of 4.5 seconds centered around t_e . For each modality, we pick $T = 16$ samples at 30 fps with a 9-frame interval, spanning a temporal window of 4.5 seconds. The resulting video and tracking streams are temporally aligned through automatic matching of UTC timestamps from the PFF FC data.

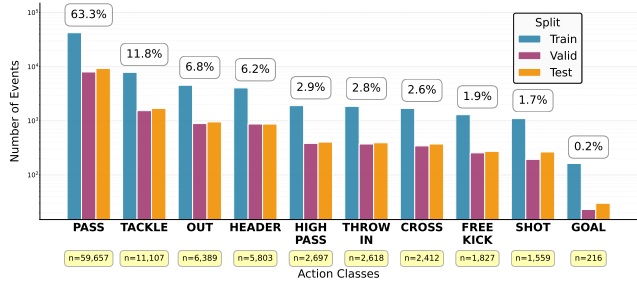


Figure 2. **Class Distribution Across Each Split.** The dataset is heavily skewed toward *PASS* (63.3%) while *GOAL* is rare (0.2%). The y-axis shows event counts; percentages denote proportions.

3.3. Statistics

The dataset contains 94,285 annotated events across 10 action classes, averaging 1,473 events per match. To avoid leakage, data were split by match: 45 training matches (66,901 events, 71%), 9 validation matches (12,865 events, 13.6%), and 10 test matches (14,519 events, 15.4%).

Class Distribution. Figure 2 shows the distribution across classes and splits. As can be seen, the dataset is highly imbalanced across classes, with *PASS* events representing 63.3% of annotations while rare events like *GOAL* account for only 0.2%. This severe imbalance (276:1 ratio) reflects the natural distribution of football events and poses significant challenges for recognition models.

Object Visibility and Tracking Quality. The tracking data maintain high completeness for players but notable incompleteness for the ball. Across all frames, 99.9% contain the full 11 players per team, with minor detection discrepancies (< 0.1%) typically occurring during substitutions. In contrast, the ball is visible in only 67.6% of frames, while the remaining 32.4% lack ball data due to occlusions (players blocking the ball, aerial challenges), broadcast camera transitions, and extreme zoom levels. This pattern reflects real-world constraints of broadcast tracking systems, where camera angles and scene dynamics naturally limit ball detection. Our tracking-based GAR methods handle missing data through sentinel values. Missing entities are assigned placeholder coordinates and excluded from graph message passing. This design allows our model to leverage agent spatial configurations, tactical formations, and motion patterns when ball information is unavailable, demonstrating robustness to incomplete observations.

3.4. Comparison with Existing Datasets

Table 1 compares our dataset with existing Group Activity Recognition benchmarks. With 94,285 annotated events, SoccerNet-GAR is the second largest GAR dataset after SoccerNet-v2 (110,458 events), and substantially larger than other football datasets: 8.5 \times larger than SoccerNet-BAS (11,041 events) and 18.2 \times larger than FIFAWC (5,196

events). Our 10 action classes overlap with the 12 classes in SoccerNet-BAS, covering the same core football events. SoccerNet-GAR is the only dataset providing synchronized tracking and video modalities for the same action instances, enabling direct apples-to-apples comparison between tracking-based and video-based approaches. This dual-modality design distinguishes our dataset from prior work as SoccerNet-v2 and SoccerNet-BAS provide only video, while existing tracking datasets lack corresponding broadcast video for the same events.

4. Methodology

4.1. Problem Formulation

We formulate Group Activity Recognition (GAR) as a multi-class classification problem over short temporal windows centered on annotated event timestamps. Given a temporal observation window of length T centered at time t_e , the model receives input from one modality, either video frames $\mathbf{X}^V = \{I_t\}_{t=1}^T$ or tracking data $\mathbf{X}^P = \{\mathcal{S}_t\}_{t=1}^T$, and predicts the collective activity label $y \in \mathcal{Y}$ from the predefined set of action classes. Formally, the task is to learn a function $f_\theta : \mathcal{X} \rightarrow \mathcal{Y}$, parameterized by θ , that predicts the class probabilities $\hat{y} = f_\theta(x)$ for a given input data $x \in \mathcal{X}$.

4.2. Classification Framework

Our classification framework follows a standard backbone-neck-head architecture [2], where modality-specific backbones extract spatial features, the neck temporally aggregates features to capture dynamics, and a classification head produces final predictions.

Video Backbones. For the video modality, we employ pretrained vision transformers [33, 34, 37, 38] that encode spatiotemporal information from broadcast footage. Given an input clip $\mathbf{X}^V = \{I_t\}_{t=1}^T$, the backbone processes each frame I_t through transformer layers with self-attention mechanisms, producing contextualized token embeddings. We extract frame-level representations $\mathbf{z}_t^V \in \mathbb{R}^{d_V}$ at each timestep t , yielding a temporal sequence $\{\mathbf{z}_t^V\}_{t=1}^T$ for subsequent temporal aggregation.

Tracking Backbone. For the tracking modality, we propose a graph-based architecture that explicitly models spatial relationships among entities at each timestep. At each frame t , we construct a graph $\mathcal{G}_t = (\mathcal{V}_t, \mathcal{E}_t)$ where nodes $\mathcal{V}_t = \{v_t^1, \dots, v_t^N\}$ represent N entities and edges \mathcal{E}_t encode their spatial interactions. A deep graph convolutional network processes these graphs to produce frame-level embeddings $\mathbf{z}_t^P \in \mathbb{R}^{d_P}$.

Classification Task. Given frame-level representations $\{\mathbf{z}_t\}_{t=1}^T$, the temporal aggregation module synthesizes information across the observation window to produce a unified representation $\hat{\mathbf{z}} = f_{\text{temp}}(\mathbf{z}_1, \dots, \mathbf{z}_T)$, where f_{temp} is a temporal aggregation function. We evaluate various tem-

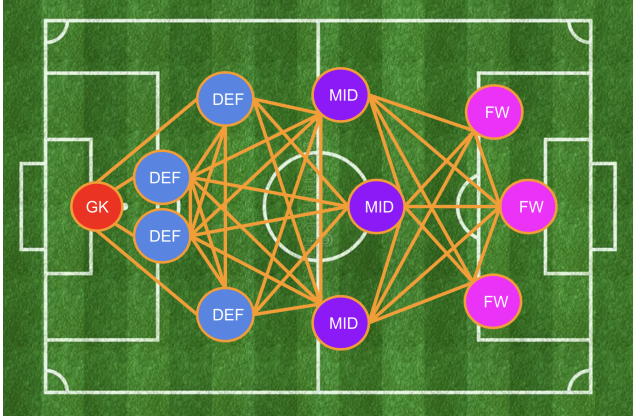


Figure 3. **Positional Graph Representation at a Single Frame.** Nodes represent players at their pitch coordinates, colored by tactical role (red: goalkeeper, blue: defenders, purple: midfielders, pink: forwards). Edges follow formation structure, connecting positionally adjacent roles within each team.

poral aggregation strategies spanning from parameter-free pooling operations to learnable sequential models. A Multi-Layer Perceptron (MLP) maps the aggregated representation to class logits through a softmax activation following $\hat{y} = \text{softmax}(\text{MLP}(\hat{z}))$.

4.3. Graph Construction

The edge set \mathcal{E}_t defines which entities exchange information during message passing. We evaluate connectivity schemes encoding different spatial interaction priors: independent processing, full connectivity, geometric proximity patterns, ball-centric interactions, and domain-informed tactical structures. These variants enable identifying which graph topologies effectively capture coordinated play.

Positional Roles. Our proposed connectivity scheme respects tactical structure based on playing positions. Players are grouped by role (goalkeeper, defender, midfielder, forward), as shown in Figure 3, using positional metadata from the tracking data. Within each team, edges connect adjacent tactical lines, reflecting typical passing patterns: goalkeeper to defenders, defenders to each other and to midfielders, midfielders to each other and to forwards, and forwards to each other. The ball connects to all entities when present. This hierarchical connectivity encodes domain knowledge about formations, passing lanes, and how possession typically progresses through defensive, midfield, and attacking phases.

5. Experiments

5.1. Experimental Setup

We benchmark different models on SoccerNet-GAR.

Tracking-based models: We employ a 20-layer Deep-

| Modality | Params | Bal. Acc. | Training Time |
|----------------------------------|--------|-----------|---------------|
| Video (VideoMAEv2, finetuned) | 86.3M | 58.1% | 34 GPU hours |
| Tracking (GIN + Attention + Pos) | 197K | 67.2% | 4 GPU hours |

Table 2. **Comparison of the Best-performing Video and Tracking Models on SoccerNet-GAR.** Tracking achieves 67.2% of balanced accuracy with $438\times$ fewer parameters and $4.25\times$ faster training than video.

GCN using GIN [42] layers with sum aggregation, ReLU, residual connections, and layer normalization. Each node projects 8-dimensional entity features to a 128-dimensional embedding. Frame-level graph representations are obtained via mean pooling and temporally aggregated with 4-head self-attention using learned positional encodings. Edges follow a positional role-based scheme connecting players by tactical roles (goalkeeper, defender, midfielder, forward). The classifier is a two-layer MLP (hidden dimension 256, output dimension 10), totaling 197K parameters. Missing entities use sentinel coordinates (-2.0 after normalization) and are excluded from graph message passing.

Video-based models: We employ VideoMAEv2-Base [38], an 86.2M-parameter transformer pretrained via masked autencoding and finetuned end-to-end. The classifier is a two-layer MLP (hidden dimension 512, output dimension 10), totaling 86.3M parameters.

Training. Tracking models use the Adam [23] with a ReduceLROnPlateau scheduler ($\text{patience} = 10$, $\text{factor} = 0.1$, $\text{min_lr} = 2 * 10^{-8}$) and initial learning rate 10^{-3} . Video models use the AdamW [29] ($\text{weight_decay} = 10^{-4}$) with ReduceLROnPlateau scheduler and initial learning rate $1e-4$. Weighted random sampling addresses class imbalance: $w_i = M/n_{y_i}$, with $M = 4000$ samples per class per epoch, ensuring balanced representation without biasing the loss. Our batch size is 32 for tracking models on a single V100 GPU; 128 for frozen video backbones on 2 V100 GPUs, 32 for full finetuning on 2 V100 GPUs, and 16 for VideoMAEv2 finetuning on 2 V100 GPUs. Data augmentation for tracking includes team flip (swap home/away labels), horizontal flip, vertical flip, and temporal jittering (\pm frames), each applied independently with $p = 0.5$; for video, we apply horizontal flip ($p = 0.5$) and color jitter ($\text{brightness} = 0.2$, $\text{contrast} = 0.2$, $\text{saturation} = 0.2$, $\text{hue} = 0.1$, $p = 0.5$). Gradient clipping ($\text{max_norm} = 1.0$) stabilizes training.

Metrics. We report balanced accuracy (average per-class recall) as the primary metric due to severe class imbalance.

5.2. Main Results: Pixels vs Positions

Table 2 presents our primary comparison between the tracking and video modalities. Our best tracking model (GIN + Attention + Positional edges) achieves 67.2% balanced accuracy using only 197K parameters, training in ap-

| Class | Samples # | Tracking | Video |
|-----------|-----------|-------------|-------------|
| PASS | 9,255 | 70.1 | 65.2 |
| TACKLE | 1,697 | 50.7 | 57.8 |
| OUT | 955 | 85.7 | 78.7 |
| HEADER | 872 | 75.0 | 55.1 |
| HIGH PASS | 405 | 27.2 | 40.5 |
| THROW IN | 393 | 65.6 | 40.5 |
| CROSS | 373 | 81.8 | 72.9 |
| FREE KICK | 273 | 86.5 | 71.1 |
| SHOT | 266 | 73.2 | 58.7 |
| GOAL | 30 | 56.7 | 36.7 |
| Overall | 14,519 | 67.2 | 57.7 |

Table 3. **Test Set Per-class Accuracy.** Tracking excels at spatially distinctive events (*e.g.*, OUT: +7.0%, FREE KICK: +15.4%, CROSS: +8.9%), and video outperforms on HIGH PASS (+13.3%) and TACKLE (+7.1%).

proximately 4 hours on a single V100 GPU. On the other hand, our best video baseline (VideoMAEv2 finetuned) achieves 58.1% balanced accuracy but requires 86.3M parameters and 34 GPU hours of training. The tracking model outperforms the video baseline by 9.1 percentage points while using $438\times$ fewer parameters and training $4.25\times$ faster. This efficiency stems from the compact representation of tracking data, where each frame consists of 23 nodes with 8-dimensional features, compared to $224\times 224\times 3$ RGB tensors for video. The performance gap suggests that explicit spatial relationships and tactical formations encoded in positions provide stronger signal than appearance cues for recognizing coordinated actions.

Per-class Analysis. Table 3 highlights complementary strengths across modalities. Tracking consistently excels on spatially distinctive events: OUT (+7.0%), FREE KICK (+15.4%), CROSS (+8.9%), GOAL (+20.0%), and SHOT (+14.5%), achieving high accuracies for events with characteristic spatial signatures (FREE KICK: 86.5%, OUT: 85.7%, CROSS: 81.8%). It struggles on spatially ambiguous actions, with HIGH PASS at only 27.2% accuracy compared to 70.1% for PASS, indicating confusion between long and short passes. Video outperforms tracking on HIGH PASS (+13.3%) and TACKLE (+7.1%), likely because visual cues such as ball trajectory and body dynamics provide discriminative information not fully captured by centroid positions. Both modalities struggle with rare classes: GOAL reaches 56.7% (tracking) and 36.7% (video) with only 30 test samples, while TACKLE remains modest at 50.7% (tracking) and 57.8% (video) despite 1,697 samples.

5.3. Ablation Studies

We evaluate design choices for both modalities. For tracking, we compare graph layer types, temporal aggregation strategies, and edge connectivity patterns. For video, we compare backbone architectures and training strategies

(frozen vs finetuned). All experiments use identical training procedures within each modality.

Video Backbone Variants. Table 4 compares four pre-trained vision backbones under two training regimes: frozen backbone with a trainable classification head versus full end-to-end finetuning. We evaluate image-pretrained models (CLIP-ViT-B, DINOv3-ViT-B) and video-pretrained models (VideoMAE-B, VideoMAEv2-B). Among frozen backbones, VideoMAEv2 performs best (47.5%), followed by DINOv3 (40.7%), CLIP (35.5%), and VideoMAE (31.4%). DINOv3 outperforms CLIP by 5.2% despite both being image-pretrained, indicating that self-supervised pretraining transfers better than contrastive vision-language pretraining for this task. Finetuning substantially improves three of four models: VideoMAE gains +26.0% (31.4% \rightarrow 57.4%), DINOv3 gains +11.7% (40.7% \rightarrow 52.4%), and VideoMAEv2 gains +10.6% (47.5% \rightarrow 58.1%). CLIP slightly declines by 1.1% (35.5% \rightarrow 34.4%), suggesting overfitting or misalignment with the classification task. VideoMAE shows the largest absolute gain but starts from the weakest frozen baseline, while VideoMAEv2 consistently achieves the best performance, highlighting the effectiveness of its video-based pretraining.

Graph Layer Variants. Table 5 compares six graph convolutional operators with MaxPool temporal aggregation and positional edges in 20-layer DeepGCN architectures with residual connections and layer normalization. GIN achieves the highest balanced accuracy (66.8%, 180K parameters), slightly surpassing GraphConv (66.7%, 174K). This suggests that the positional edge structure provides most of the discriminative signal, with the choice of aggregation operator having minimal impact. More complex operators underperform: GATv2 reaches 61.3% (-5.5 vs. GIN) and EdgeConv achieves 58.7% (-8.1), failing on specific classes (EdgeConv: HIGH PASS 6.9%, OUT 55.4%; GATv2: THROW IN 20.4%). GraphSAGE (65.6%) and GEN (66.3%) achieve competitive overall performance but require $1.9\times$ – $2.3\times$ more parameters than GIN. Per-class results reveal substantial variability: GATv2 excels on HIGH PASS (69.3% vs GIN 27.2%), while GraphSAGE performs best on THROW IN (81.6%) but fails on HIGH PASS (4.0%), indicating that different operators capture different spatial relationships, though none consistently outperform the simpler GIN.

Temporal Aggregation. Table 6 compares five temporal aggregation strategies with GIN layers and positional edges over the 4.5-second observation window. Attention achieves the highest balanced accuracy (67.2%), only slightly above MaxPool (66.8%, +0.4) despite higher complexity (197K vs 180K params), indicating that peak spatial configurations dominate over detailed temporal modeling. BiLSTM (66.0%, 350K) and TCN (65.0%, 205K) underperform, while Average Pooling is substantially worse

| Backbone | Frozen | Params | Bal. Acc. | Cross | Free Kick | Goal | Header | High Pass | Out | Pass | Tackle | Shot | Throw In |
|--------------|--------|--------|-----------|-------|-----------|------|--------|-----------|------|------|--------|------|----------|
| CLIP-ViT-B | ✓ | 85.8M | 35.5 | 41.3 | 46.9 | 46.7 | 18.2 | 23.5 | 31.3 | 53.3 | 23.0 | 50.4 | 20.6 |
| CLIP-ViT-B | ✗ | 85.8M | 34.4 | 59.0 | 38.5 | 36.7 | 22.5 | 17.5 | 28.5 | 37.0 | 6.0 | 40.2 | 58.5 |
| DINOv3-ViT-B | ✓ | 85.7M | 40.7 | 55.5 | 54.6 | 36.7 | 25.2 | 32.1 | 36.9 | 50.0 | 28.2 | 51.1 | 36.9 |
| DINOv3-ViT-B | ✗ | 85.7M | 52.4 | 67.3 | 75.5 | 3.3 | 61.0 | 38.8 | 63.7 | 64.1 | 33.7 | 69.2 | 47.8 |
| VideoMAE-B | ✓ | 86.3M | 31.4 | 31.6 | 42.5 | 33.3 | 33.3 | 16.5 | 30.7 | 48.5 | 10.8 | 42.9 | 23.7 |
| VideoMAE-B | ✗ | 86.3M | 57.4 | 67.6 | 64.8 | 36.7 | 67.0 | 84.4 | 78.1 | 66.5 | 40.0 | 68.1 | 1.0 |
| VideoMAEv2-B | ✓ | 86.3M | 47.5 | 61.4 | 63.0 | 56.7 | 43.5 | 24.9 | 44.1 | 52.8 | 28.6 | 48.9 | 51.7 |
| VideoMAEv2-B | ✗ | 86.3M | 58.1 | 71.1 | 67.4 | 30.0 | 63.2 | 67.9 | 75.9 | 68.5 | 46.8 | 69.6 | 20.6 |

Table 4. **Video Backbone Ablation.** Finetuning substantially improves over frozen backbones (+26.0% for VideoMAE, +11.7% for DINOv3, +10.6% for VideoMAEv2). VideoMAEv2 finetuned achieves the best video performance (58.1%). CLIP’s performance decreases with finetuning (−1.1%), suggesting its vision-language pretraining does not provide useful inductive biases for this task.

| Backbone | Params | Bal. Acc. | Cross | Free Kick | Goal | Header | High Pass | Out | Pass | Tackle | Shot | Throw In |
|------------|-------------|-------------|-------|-----------|------|--------|-----------|------|------|--------|------|----------|
| GraphConv | 174K | 66.7 | 82.7 | 83.6 | 71.1 | 73.6 | 28.3 | 84.2 | 74.0 | 44.8 | 65.4 | 59.1 |
| GATv2 | 177K | 61.3 | 85.0 | 61.2 | 80.0 | 70.4 | 69.3 | 82.4 | 61.3 | 35.0 | 48.3 | 20.4 |
| GraphSAGE | 421K | 65.6 | 77.5 | 82.8 | 70.0 | 71.1 | 4.0 | 83.0 | 76.3 | 44.0 | 66.0 | 81.6 |
| EdgeConv | 174K | 58.7 | 81.2 | 60.1 | 76.7 | 76.3 | 6.9 | 55.4 | 50.0 | 39.9 | 60.4 | 79.9 |
| GEN | 341K | 66.3 | 84.7 | 85.4 | 53.3 | 71.7 | 21.3 | 82.3 | 76.2 | 44.2 | 74.7 | 68.9 |
| GIN | 180K | 66.8 | 81.8 | 82.2 | 69.5 | 73.0 | 27.7 | 85.1 | 72.4 | 48.1 | 65.7 | 62.5 |

Table 5. **Graph Layer Ablation with MaxPool and Positional Edges.** GIN achieves the best balanced accuracy with 180K parameters. GraphConv performs nearly identically, suggesting simple message passing suffices when positional structure is explicitly encoded.

(60.1%), confirming unequal frame contributions. Per-class patterns vary: TCN fails on GOAL (26.7%) despite strong SHOT (80.0%), AvgPool achieves highest GOAL accuracy (83.3%), and BiLSTM excels at TACKLE (58.5%) but struggles on HIGH PASS (20.1%). Attention maintains the best overall balanced accuracy through consistent, if not peak, per-class performance.

Edge Connectivity. Table 7 compares seven connectivity patterns with GIN layers and MaxPool aggregation. Positional edges perform best (66.8%), surpassing no-edges (62.0%), showing that tactical spatial connections aid coordinated action recognition. Most geometric patterns underperform: Distance $r = 15$ (59.4%), Ball Distance $r = 20$ (59.9%), Ball KNN $k = 8$ (60.6%), KNN $k = 8$ (61.1%), and Fully Connected (61.4%), suggesting unrestricted or proximity-based edges dilute discriminative structure. Per-class results highlight extreme variance: Distance $r = 15$ achieves top HIGH PASS (81.7%) but fails on THROW IN (6.1%), no-edges excels on HEADER (79.0%), and positional edges provide largest gains on OUT (85.1% vs 59.6%) and TACKLE (48.1% vs 36.4%), highlighting the value of encoding tactical structure.

6. Analysis

Model Parameters vs. Balanced Accuracy. Figure 4 compares parameter efficiency across all evaluated models. Tracking models achieve 58.7%–67.2% balanced accuracy with 174K–421K parameters, while video mod-

els achieve 31.4%–58.1% with 85.7M–86.3M parameters. Our best model (GIN + Attention, 197K params, 67.2%) outperforms the best video baseline (VideoMAEv2 finetuned, 86.3M params, 58.1%) by 9.1 percentage points while using 438× fewer parameters. Tracking models exhibit clear clustering by component type. Backbone variants span 174K–421K parameters with 58.7%–66.8% accuracy, where GraphSAGE (421K) uses 2.3× more parameters than GIN (180K) but underperforms by 1.2. Temporal aggregation methods cluster tightly at 180K–350K parameters with 60.1%–67.2% accuracy, where BiLSTM (350K) uses 1.8× more parameters than Attention (197K) but achieves 1.2 lower accuracy. Video models cluster at ∼86M parameters with accuracy varying by 26.7 (31.4%–58.1%). This large variance stems from pretraining strategy and frozen vs finetuned backbones rather than architectural differences. VideoMAE finetuned (86.3M, 57.4%) and CLIP frozen (85.8M, 35.5%) have nearly identical parameter counts but differ by 21.9% in accuracy, demonstrating that parameter count alone does not determine performance for video models.

Data Scaling. Figure 5 shows performance versus training set size for both modalities. Tracking achieves 59.8% with only 5 matches and plateaus around 40 matches (67.0%), while video achieves 42.7% with 5 matches and continues improving to 58.1% at 45 matches. The 17.1% gap at 5 matches narrows to 8.7% at 45 matches, indicating video benefits more from additional data. However, track-

| Temporal | Params | Bal. Acc. | Cross | Free Kick | Goal | Header | High Pass | Out | Pass | Tackle | Shot | Throw In |
|------------------|-------------|-------------|-------|-----------|------|--------|-----------|------|------|--------|------|----------|
| AvgPool | 180K | 60.1 | 74.0 | 74.7 | 83.3 | 64.5 | 15.4 | 56.1 | 55.3 | 39.6 | 65.7 | 71.9 |
| MaxPool | 180K | 66.8 | 81.8 | 82.2 | 69.5 | 73.0 | 27.7 | 85.1 | 72.4 | 48.1 | 65.7 | 62.5 |
| TCN | 205K | 65.0 | 84.2 | 85.7 | 26.7 | 71.3 | 27.2 | 85.5 | 74.5 | 52.8 | 80.0 | 61.7 |
| BiLSTM | 350K | 66.0 | 84.2 | 81.3 | 50.0 | 68.9 | 20.1 | 84.1 | 67.2 | 58.5 | 75.5 | 69.9 |
| Attention | 197K | 67.2 | 81.8 | 86.5 | 56.7 | 75.0 | 27.2 | 85.7 | 70.1 | 50.7 | 73.2 | 65.6 |

Table 6. **Temporal Aggregation Ablation with GIN and Positional Edges.** Attention achieves the best balanced accuracy (67.2%) but only marginally outperforms MaxPool (66.8%), indicating peak spatial configurations dominate temporal dynamics.

| Edge Type | Params | Bal. Acc. | Cross | Free Kick | Goal | Header | High Pass | Out | Pass | Tackle | Shot | Throw In |
|-----------------------|-------------|-------------|-------|-----------|------|--------|-----------|------|------|--------|------|----------|
| No Edges | 180K | 62.0 | 81.2 | 78.8 | 70.0 | 79.0 | 27.2 | 59.6 | 59.2 | 36.4 | 69.8 | 58.4 |
| Fully Connected | 180K | 61.4 | 82.3 | 78.4 | 73.3 | 80.1 | 13.1 | 57.6 | 47.8 | 37.8 | 65.7 | 78.1 |
| Ball Distance (r=20m) | 180K | 59.9 | 85.5 | 72.9 | 66.7 | 77.9 | 14.6 | 58.3 | 50.3 | 35.2 | 66.0 | 71.9 |
| Ball KNN (k=8) | 180K | 60.6 | 81.0 | 68.9 | 80.0 | 78.8 | 9.4 | 56.5 | 53.5 | 35.6 | 65.3 | 77.0 |
| Distance (r=15m) | 180K | 59.4 | 85.8 | 72.2 | 80.0 | 74.4 | 81.7 | 56.6 | 50.4 | 28.2 | 58.1 | 6.1 |
| KNN (k=8) | 180K | 61.1 | 83.9 | 74.0 | 73.3 | 78.8 | 14.9 | 57.4 | 49.7 | 36.1 | 67.2 | 75.5 |
| Positional | 180K | 66.8 | 81.8 | 82.2 | 69.5 | 73.0 | 27.7 | 85.1 | 72.4 | 48.1 | 65.7 | 62.5 |

Table 7. **Edge Connectivity Ablation with GIN and MaxPool.** Positional edges outperform all alternatives. Independent node processing outperforms geometric proximity patterns, showing that poorly chosen edges introduce noise.

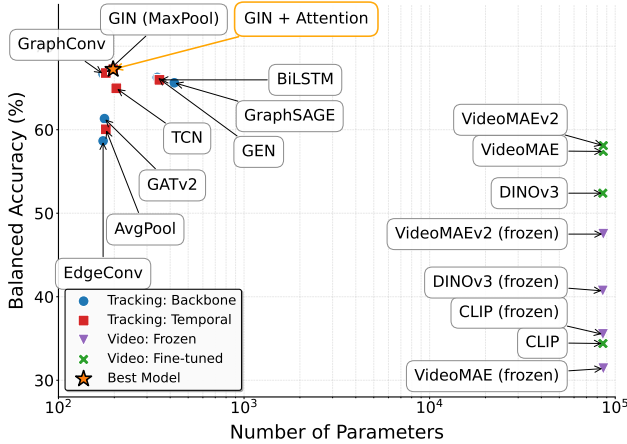


Figure 4. **Balanced Accuracy vs. Parameter Count.** Tracking models achieve 67.2% with 197K parameters, outperforming video models (58.1%, 86.3M params) by 9.1 while using 438× fewer parameters.

ing maintains superior performance across all data regimes while plateauing earlier, suggesting structured positional representations require less training data to reach peak performance.

7. Conclusion

We introduced SoccerNet-GAR, a benchmark for group activity recognition that pairs broadcast video with tracking data under match-level splits. Our evaluation reveals that tracking models achieve 67.2% balanced accuracy with 197K parameters, outperforming video models (58.1%,

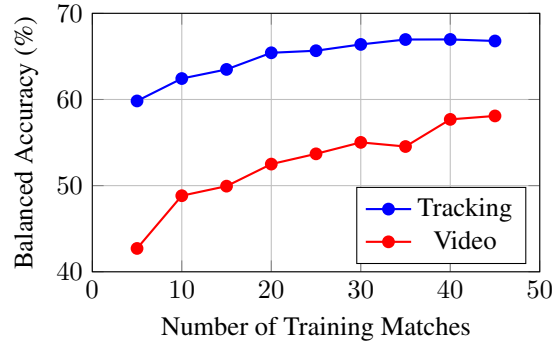


Figure 5. **Performance vs. Number of Training Matches for Video and Tracking Modalities.** Tracking achieves higher accuracies across all data regimes and plateaus earlier (≈ 35 matches), while video does not. The gap narrows from 15.8% (5 matches) to 8.7% (45 matches).

86.3M parameters) by 9.1% while using 438× fewer parameters and training 4.25× faster. Our ablation studies demonstrate that domain-informed graph construction (positional edges encoding tactical structure) substantially outperforms geometric proximity patterns (+5.4%), while complex temporal models provide minimal gains over simple max pooling (+0.4% for attention). Tracking excels on spatially distinctive events (OUT, FREE KICK, CROSS) but struggles with HIGH PASS, where video outperforms by 13.3%, suggesting complementary strengths. Our findings indicate that explicit encoding of spatial relationships provides stronger signal than appearance cues for recognizing coordinated actions in this domain. However, per-class

analysis reveals modality-specific strengths, motivating future work on multimodal fusion that combines positional structure with visual appearance. Our dataset and benchmark provide a foundation for advancing multimodal research in group activity recognition.

References

- [1] Timur Bagautdinov, Alexandre Alahi, François Fleuret, Pascal Fua, and Silvio Savarese. Social scene understanding: End-to-end multi-person action localization and collective activity recognition. In *CVPR*, pages 4315–4324, 2017. [2](#)
- [2] Yassine Benzakour, Bruno Cabado, Silvio Giancola, Anthony Cioppa, Bernard Ghanem, and Marc Van Droogenbroeck. Osl-actionspotting: A unified library for action spotting in sports videos, 2024. [4](#)
- [3] Shaked Brody, Uri Alon, and Eran Yahav. How attentive are graph attention networks?, 2022. [3](#)
- [4] Alejandro Cartas, Coloma Ballester, and Gloria Haro. A graph-based method for soccer action spotting using unsupervised player classification. In *ACM International Workshop on Multimedia Content Analysis in Sports (MMSports)*, pages 93–102, 2022. [2](#)
- [5] Wongun Choi, Khuram Shahid, and Silvio Savarese. What are they doing?: Collective activity classification using spatio-temporal relationship among people. In *2009 IEEE 12th international conference on computer vision workshops, ICCV Workshops*, pages 1282–1289. IEEE, 2009. [2](#), [3](#)
- [6] Anthony Cioppa, Adrien Deliege, Silvio Giancola, Bernard Ghanem, and Marc Van Droogenbroeck. Scaling up soccer-net with multi-view spatial localization and re-identification. *Scientific data*, 9(1):355, 2022. [2](#)
- [7] Anthony Cioppa, Adrien Deliège, Silvio Giancola, Floriane Magera, Olivier Barnich, Bernard Ghanem, and Marc Van Droogenbroeck. Camera calibration and player localization in SoccerNet-v2 and investigation of their representations for action spotting, pages 4532–4541, June 2021. [2](#)
- [8] Anthony Cioppa, Silvio Giancola, Vladimir Somers, Floriane Magera, Xin Zhou, Hassan Mkhallati, Adrien Deliège, Jan Held, Carlos Hinojosa, Amir M Mansourian, et al. SoccerNet 2023 challenges results. *Sports Engineering*, 27(2):24, 2024. [2](#), [3](#)
- [9] Yifu Cui, Chenkai Zeng, Xiaoyu Zhao, Yiyao Yang, Gangshan Wu, and Limin Wang. SportsMOT: A large multi-object tracking dataset in multiple sports scenes. In *Advances in Neural Information Processing Systems (NeurIPS)*, volume 36, 2023. [2](#)
- [10] Adrien Deliège, Anthony Cioppa, Silvio Giancola, Meisam J Seikavandi, Jacob V Dueholm, Kamal Nasrollahi, Bernard Ghanem, Thomas B Moeslund, and Marc Van Droogenbroeck. SoccerNet-v2: A dataset and benchmarks for holistic understanding of broadcast soccer videos. In *IEEE Conference on Computer Vision and Pattern Recognition Workshops (CVPRW)*, pages 4508–4519, 2021. [2](#), [3](#)
- [11] Dawei Ding and Hsiangsheng Huang. A graph attention based approach for trajectory prediction in multi-agent sports games. *arXiv preprint arXiv:2012.10531*, 2020. [3](#)
- [12] Hao-Shu Fang, Yuanlu Xu, Wenguan Wang, Xiaobai Liu, and Song-Chun Zhu. Learning pose grammar to encode human body configuration for 3d pose estimation. In *Proceedings of the AAAI conference on artificial intelligence*, volume 32, 2018. [2](#), [3](#)
- [13] Javier Fernández, Luke Bornn, and Dan Cervone. Wide open spaces: A statistical technique for measuring space creation in professional soccer. In *MIT Sloan Sports Analytics Conference*, 2019. [2](#)
- [14] Nuno C Garcia, Pietro Morerio, and Vittorio Murino. Compositional action recognition with dependent compositional attention. In *CVPRW*, pages 668–669, 2020. [2](#)
- [15] Kirill Gavrilyuk, Ryan Sanford, Mehrsan Javan, and Cees GM Snoek. Actor-transformers for group activity recognition. In *IEEE Conference on Computer Vision and Pattern Recognition (CVPR)*, pages 839–848, 2020. [2](#), [3](#)
- [16] Silvio Giancola, Mohieddine Amine, Tarek Dghaily, and Bernard Ghanem. SoccerNet: A scalable dataset for action spotting in soccer videos. In *IEEE Conference on Computer Vision and Pattern Recognition Workshops (CVPRW)*, pages 1711–1721, 2018. [2](#), [3](#)
- [17] Alex Graves and Jürgen Schmidhuber. Framewise phoneme classification with bidirectional lstm and other neural network architectures. *Neural networks*, 18(5-6):602–610, 2005. [3](#)
- [18] Will Hamilton, Zhitao Ying, and Jure Leskovec. Inductive representation learning on large graphs. In *Advances in Neural Information Processing Systems (NeurIPS)*, pages 1024–1034, 2017. [3](#)
- [19] James Hong, Haotian Zhang, Michaël Gharbi, Matthew Fisher, and Kayvon Fatahalian. Spotting temporally precise, fine-grained events in video. In *European Conference on Computer Vision*, pages 33–51. Springer, 2022. [2](#)
- [20] Mostafa S Ibrahim, Srikanth Muralidharan, Zhiwei Deng, Arash Vahdat, and Greg Mori. A hierarchical deep temporal model for group activity recognition. In *Proceedings of the IEEE conference on computer vision and pattern recognition*, pages 1971–1980, 2016. [2](#), [3](#)
- [21] Christian Ingwersen and Joni-Kristian Kämäriäinen. SportsPose: A dynamic 3d sports pose dataset. In *IEEE Conference on Computer Vision and Pattern Recognition Workshops (CVPRW)*, 2023. [2](#)
- [22] Dongkeun Kim, Youngkil Song, Minsu Cho, and Suha Kwak. Towards more practical group activity detection: A new benchmark and model. *arXiv preprint arXiv:2312.02878*, 2023. [3](#)
- [23] Diederik P Kingma. Adam: A method for stochastic optimization. *arXiv preprint arXiv:1412.6980*, 2014. [5](#)
- [24] Thomas N Kipf and Max Welling. Semi-supervised classification with graph convolutional networks. In *International Conference on Learning Representations (ICLR)*, 2017. [3](#)
- [25] Colin Lea, Michael D Flynn, Rene Vidal, Austin Reiter, and Gregory D Hager. Temporal convolutional networks for action segmentation and detection. In *IEEE Conference on Computer Vision and Pattern Recognition (CVPR)*, pages 156–165, 2017. [3](#)
- [26] Guohao Li, Matthias Muller, Ali Thabet, and Bernard Ghanem. DeepGCNs: Can GCNs go as deep as CNNs? In

IEEE International Conference on Computer Vision (ICCV), pages 9267–9276, 2019. 3

[27] Shuaicheng Li, Qianggang Cao, Lingbo Liu, Kunlin Yang, Shinan Liu, Jun Hou, and Shuai Yi. Groupformer: Group activity recognition with clustered spatial-temporal transformer. In *ICCV*, pages 13668–13677, 2021. 2

[28] Zhengcen Li, Xianxiang Chang, Yueran Li, and Jing Su. Skeleton-based group activity recognition via spatial-temporal panoramic graph. In *ECCV*, pages 254–270. Springer, 2024. 2

[29] Ilya Loshchilov and Frank Hutter. Decoupled weight decay regularization. *arXiv preprint arXiv:1711.05101*, 2017. 5

[30] Abdul Majeed, Mohammad Farukh Hashmi, Muhammad Umar Ashraf, Gitanjali Srivastava, Zong Woo Geem, and Neeraj Dhanraj Bokde. Real-time analysis of soccer ball-player interactions using graph convolutional networks for enhanced game insights. *Scientific Reports*, 15(1):1–19, 2025. 3

[31] Duoxuan Pei, Di Huang, and Yunhong Wang. Fifawc: a dataset with detailed annotation and rich semantics for group activity recognition. *Frontiers of Computer Science*, 18(6):186351, 2024. 3

[32] PFF FC. Data-driven exploration of the 2022 fifa world cup. <https://www.blog.fc.pff.com/blog/enhanced-2022-world-cup-dataset>, 2023. Accessed: November 12, 2025. 3

[33] Alec Radford, Jong Wook Kim, Chris Hallacy, Aditya Ramesh, Gabriel Goh, Sandhini Agarwal, Girish Sastry, Amanda Askell, Pamela Mishkin, Jack Clark, et al. Learning transferable visual models from natural language supervision. In *International conference on machine learning*, pages 8748–8763. PMLR, 2021. 2, 4

[34] Oriane Siméoni, Huy V Vo, Maximilian Seitzer, Federico Baldassarre, Maxime Oquab, Cijo Jose, Vasil Khalidov, Marc Szafraniec, Seungeun Yi, Michaël Ramamonjisoa, et al. Dinov3. *arXiv preprint arXiv:2508.10104*, 2025. 2, 4

[35] João V Carvalho Soares, Mubarak Shah, and Ralph Ewerth. Temporally precise action spotting in soccer videos using dense detection anchors. In *Proceedings of the IEEE/CVF Conference on Computer Vision and Pattern Recognition Workshops*, pages 5074–5085, 2023. 2

[36] Vladimir Somers, Victor Joos, Anthony Cioppa, Silvio Giancola, Seyed Abolfazl Ghasemzadeh, Floriane Magera, Baptiste Standaert, Amir Mohammad Mansourian, Xin Zhou, Shohreh Kasaei, et al. SoccerNet game state reconstruction: End-to-end athlete tracking and identification on a minimap. In *IEEE Conference on Computer Vision and Pattern Recognition Workshops (CVPRW)*, 2024. 2

[37] Zhan Tong, Yibing Song, Jue Wang, and Limin Wang. Videomae: Masked autoencoders are data-efficient learners for self-supervised video pre-training. *Advances in neural information processing systems*, 35:10078–10093, 2022. 2, 4

[38] Limin Wang, Bingkun Huang, Zhiyu Zhao, Zhan Tong, Yinan He, Yi Wang, Yali Wang, and Yu Qiao. Videomae v2: Scaling video masked autoencoders with dual masking. In *Proceedings of the IEEE/CVF conference on computer vision and pattern recognition*, pages 14549–14560, 2023. 2, 4, 5

[39] Yue Wang, Yongbin Sun, Ziwei Liu, Sanjay E Sarma, Michael M Bronstein, and Justin M Solomon. Dynamic graph CNN for learning on point clouds. In *ACM Transactions on Graphics (TOG)*, volume 38, pages 1–12, 2019. 3

[40] Artur Xarles, Sergio Escalera, Thomas B Moeslund, and Albert Clapés. ASTRA: An action spotting transformer for soccer videos. *arXiv preprint arXiv:2404.01891*, 2024. 2

[41] Artur Xarles, Sergio Escalera, Thomas B Moeslund, and Albert Clapés. T-deed: Temporal-discriminability enhancer encoder-decoder for precise event spotting in sports videos. In *Proceedings of the IEEE/CVF Conference on Computer Vision and Pattern Recognition*, pages 3410–3419, 2024. 2

[42] Keyulu Xu, Weihua Hu, Jure Leskovec, and Stefanie Jegelka. How powerful are graph neural networks?, 2019. 3, 5

[43] Rui Yan, Lingxi Xie, Jinhui Tang, Xiangbo Shu, and Qi Tian. Social adaptive module for weakly-supervised group activity recognition, 2020. 3

[44] Sijie Yan, Yuanjun Xiong, and Dahua Lin. Spatial temporal graph convolutional networks for skeleton-based action recognition. In *AAAI*, volume 32, 2018. 2, 3

[45] Raymond A Yeh, Alexander G Schwing, Jonathan Huang, and Kevin Murphy. Forecasting basketball trajectories and player intentions using graph neural networks. In *ICML Workshop on Computer Vision for Autonomous Vehicles*, 2019. 2, 3

[46] Hangjie Yuan and Dong Ni. Learning visual context for group activity recognition. In *AAAI*, volume 34, pages 3261–3269, 2021. 2

[47] Honglu Zhou, Asim Kadav, Aviv Shamsian, Shijie Geng, Farley Lai, Long Zhao, Ting Liu, Mubbashir Kapadia, and Hans Peter Graf. Composer: Compositional reasoning of group activity in videos with keypoint-only modality. In *ECCV*, pages 249–266. Springer, 2022. 2